Receptor Noise and Directional Sensing in Eukaryotic Chemotaxis

Wouter-Jan Rappel and Herbert Levine

Center for Theoretical Biological Physics, University of California, San Diego, La Jolla, California 92093-0319, USA
(Received 7 January 2008; published 2 June 2008)

Chemotacting eukaryotic cells are able to detect very small chemical gradients (~1%) for a large range of background concentrations. For these chemical environments, fluctuations in the number of bound ligands will become important. Here, we investigate the effect of receptor noise in a simplified one-dimensional geometry. The auto- and cross-correlations of the noise sources at the front and the back of the cell are explicitly computed using an effective Monte Carlo simulation tool. The resulting stochastic equations for the investigated directional sensing model can be solved analytically in Fourier space. We determine the chemotactic efficiency, a measure of motility for the cell, as a function of several experimental parameters, leading to explicit experimental predictions.

Chemotaxis, the directed movement of cells in response to external chemical gradients, plays an important role in a wide variety of biological processes including wound healing, fetal development, and cancer metastasis [1]. The externally diffusing chemoattractant molecules (ligands) bind to cell membrane receptors which activate second messenger signaling pathways. In the case of eukaryotic cells, the subject of this Letter, these pathways eventually leads to cell motion in the form of crawling up the gradient.

Surprisingly, eukaryotic cells have been found to chemotax in gradients that are only 1%–2% across the cell body. Furthermore, *Dictyostelium* discoideum cells, a social amoeba, were found to be able to direct their motion even when the average external chemoattractant concentration was well below the dissociation constant K_d (the value for which half the receptors are bound in equilibrium) [2]. In fact, at threshold the difference in the number of bound receptors at the front and the back can be estimated to be on the order of 20 while the total number of bound receptors is only a few hundred. This immediately raises the question of the effect of noise on chemotaxis, a topic that has been studied previously using a variety of approximative techniques [3–6]. What has been lacking, however, is a formalism that simulates quantitatively the receptor noise and its correlations and uses this as input for an intracellular chemotactic model.

In this Letter, we will address the role of receptor noise in directional sensing, the first step in chemotaxis during which cells determine the direction of the gradient. We will use a simplified one-dimensional geometry, schematically shown in Fig. 1, which allows us to obtain analytical expressions for the diffusive part of the directional sensing model. Our 1D cell contains a front and a back, both considers to be points, connected by a line, representing the interior, or cytosol, of the cell. The input S at the front and back of the cell represents the number of bound receptors arising from the simple ligand-receptor interaction $L + R_0 \rightleftharpoons R_1$. The forward rate $k_+[L]$, where $[L]$ represents the ligand concentration, and backward rate k_- determine the transitions between the unoccupied R_0

and occupied R_1 states and can be combined to give the dissociation constant $K_d \equiv \frac{k_-}{k_+}$. We will assume that the cell is placed in a gradient of steepness p and midpoint concentration c such that the concentration at the front (f) is given by $c_f = c(1 + p)$ and at the back (b) by $c_b = c(1 - p)$ [7]. The signal S at the front and back can then be written as the sum of a deterministic and a stochastic part:

$$S_f = \frac{c(1 + p)}{c(1 + p) + K_d} + \eta_f;$$
$$S_b = \frac{c(1 - p)}{c(1 - p) + K_d} + \eta_b. \tag{1}$$

Here, η_f and η_f are noise sources with auto and cross correlations given by $<\eta_f(t)\eta_f(t')> = C_{ff}(t - t')$, $<\eta_b(t)\eta_b(t')> = C_{bb}(t - t')$ and $<\eta_f(t)\eta_b(t')> = C_{fb}(t - t')$ which arise due to the stochastic nature of the binding or unbinding process as well as the diffusive process of the ligands.

The input S needs to be coupled to a directional sensing mechanism which translates the external asymmetry to an internal asymmetry. A number of different mechanisms have been proposed including Turing-type instability mechanisms [8], phase separation mechanisms [9] and depletion mechanisms [10,11]. Here, we will use the recently developed balanced inactivation model [12], which has as the key feature a cytosolic diffusing inhibitory species, denoted here by B. This inhibitor, postulated in almost all directional sensing studies including local excitation-global inhibition models [13,14], obeys the standard diffusion equation $\frac{\partial B}{\partial t} = D\nabla^2 B$, where D is the diffu-
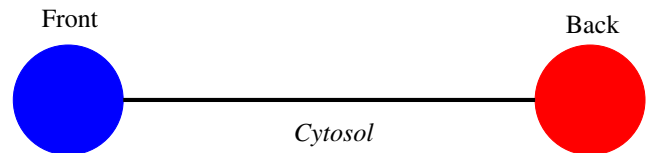
Front   Back

Cytosol

FIG. 1 (color online).   Schematic representation of our one-dimensional cell.

sion constant of the inhibitor. B is linearly generated by the signal S at a rate k_a and binds to the membrane at a rate k_b: $D\frac{\partial B}{\partial n} = k_a S - k_b B$. The membrane-bound version of B can inactivate a membrane-bound activator A which functions as the readout component of the model and which is also generated at a rate k_a. If the diffusion of the cytosolic inhibitor is fast enough the levels of membrane-bound B at the front and the back are nearly identical. This leads to an almost complete inactivation of A at the back while the level A at the front remains significantly nonzero. The resulting large asymmetry in A can be achieved over a wide range of gradient and model parameters. Further details of this model can be found in the original Ref. [12]. It should be noted that many of the biochemical components in directional sensing models have not yet been identified. One cannot, therefore, make an *a priori* estimate for the additional noise resulting from the finite concentration of the signaling pathway components. Here, we treat the directional sensing model deterministically and our results should be viewed as an upper bound on the gradient detection capability.

The linear relationship between B and S allows us to analytically solve the diffusion equation in Fourier space. Let us write the solution of B as a sum of a deterministic part and a stochastic part: $B_f = B_{f,0} + b_f$ and $B_b = B_{b,0} + b_b$. Explicit expressions can be obtained for the deterministic part [12] and the stochastic part has as correlation function $\langle b_f(t) b_f(t') \rangle = N_{ff}(t - t')$ with similar expressions for N_{bb} and N_{fb}. Then, in Fourier space we find

$$\tilde{B}(x, \omega) = \tilde{b}_e(\omega)\frac{\cosh(\kappa \mathrm{x})}{\cosh(\kappa \mathrm{L}/2)} + \tilde{b}_o(\omega)\frac{\sinh(\kappa \mathrm{x})}{\sinh(\kappa \mathrm{L}/2)}, \quad (2)$$

where $\kappa = \sqrt{-i\omega/D}$ and where we have introduced the tilde to denote a quantity in Fourier space. Plugging this into the boundary conditions, we find that $\tilde{b}_e = k_a(\tilde{\eta}_f + \tilde{\eta}_b)/\{2[k_b + D\kappa\tanh(\kappa L/2)]\}$ and a similar expression for $\tilde{b}_o$. It is easy to verify that $\tilde{b}_f = \tilde{b}_e + \tilde{b}_o$ and $\tilde{b}_b = \tilde{b}_e - \tilde{b}_o$, from which we can find (lengthy) expressions for the correlation spectra which are functions of the correlation functions of the external signal. For example, for the front-front correlation spectrum we find

$$\tilde{N}_{ff}(\omega) = \frac{k_a^2}{4}\left(\tilde{C}_{ff}(\omega)\left[\frac{1}{k_b + D\kappa\tanh(\kappa\mathrm{L}/2)} + \frac{1}{k_b + D\kappa\coth(\kappa\mathrm{L}/2)}\right]^2\right.$$
$$+ \tilde{C}_{bb}(\omega)\left[\frac{1}{k_b + D\kappa\tanh(\kappa\mathrm{L}/2)} - \frac{1}{k_b + D\kappa\coth(\kappa\mathrm{L}/2)}\right]^2 + \tilde{C}_{fb}(\omega)\left[\frac{1}{k_b + D\kappa\tanh(\kappa\mathrm{L}/2)} + \frac{1}{k_b + D\kappa\coth(\kappa\mathrm{L}/2)}\right]$$
$$\left.\times\left[\frac{1}{k_b + D\kappa\tanh(\kappa\mathrm{L}/2)} - \frac{1}{k_b + D\kappa\coth(\kappa\mathrm{L}/2)}\right]^* + \mathrm{c.c.}\right),$$

where c.c. stands for the complex conjugate of the last term in the right-hand side expression.

To obtain the spectra of the correlation functions C_{ff}, C_{bb} and C_{fb}, we use MCELL3, a modeling tool for realistic simulations of cellular signaling in complex three dimensional geometries [15]. This simulation tool, recently used by us to determine the autocorrelation function for a spherical cell [16], uses highly optimized Monte Carlo algorithms to track the stochastic behavior of discrete molecules in space and time as they diffuse in user-specified geometries. It can model interactions between diffusing molecules and receptors on cell membranes as well as molecule-molecule interactions and has been validated extensively [15].

In our MCell simulations, we placed receptors uniformly on the surface of a sphere that was in a much larger computational box. We divided the cell into two halves and the receptors in one half of the cell were occupied according to the equilibrium value $\frac{N}{2}\frac{c}{c+K_d}$ while the other half contained empty receptors. The boundary of the box is taken to be absorptive so once a ligand hits the boundary it is removed from the system. The simulation recorded the total number of bound receptors in each half of the cell as a function of time from which the auto and cross correlation were calculated. This method, also applied in [16], is computationally much more efficient than recording the

number of bound receptors in a constant background concentration and produces accurate results for the correlation times. Furthermore, it also allows us to estimate the amplitude of the cross correlation. Of course, since the receptors on the second half of the cell are initially all empty the probability of binding to the second half is slightly larger than for a uniformly occupied sphere, leading to an overestimation of cross correlation. However, for small concentrations this effect is negligible and the numerically obtained amplitude is accurate.

To obtain a statistically meaningful answer we ran this simulation 100 times and examples of the result can be seen in Figs. 2(a) and 2(b) for the auto and cross correlation, respectively. As in Ref. [16], we found that the autocorrelation can be fitted accurately by a decaying exponential $C_{ff} = A_a(c_f)e^{-t/\tau_a}$, where the amplitude is given by the variance of a single receptor ($A_a(c_f) = N c_f K_d/(2(c_f + K_d)^2)$), and with an autocorrelation time given by

$$\tau_a = \frac{1}{k_- + k_+ c_f} + \frac{N}{8\pi D_l R K_d} \equiv \tau_{\mathrm{rec}} + \tau_{\mathrm{diff}}. \quad (3)$$

Here, τ_{rec} describes the receptor dynamics and τ_{diff} describes the contribution of ligand diffusion (D_l is the diffusion constant of the ligands and R is the radius of
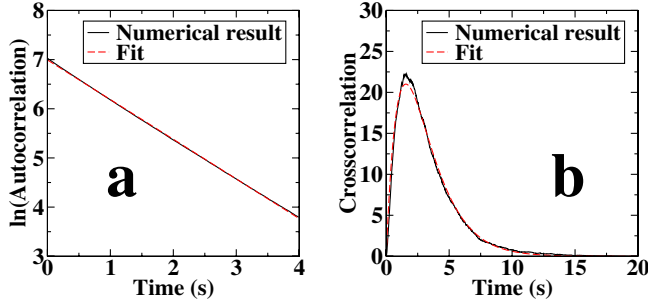
FIG. 2 (color online). The auto (a) and cross correlation (b) for a semisphere computed using MCell. The red curves are the fits using the formulas from the main text with as results: $A_c = 37$, $\tau_c = 1.56$ s and $\tau_a = 1.15$ s. Parameters are based on data from *Dictyostelium*: $N = 70\,000$ receptors, $D_l = 200$ μm^2/s, $R = 5$ μm, $k_- = 1/s$ and $K_d = 30$ nM with $c = 1$ nM.
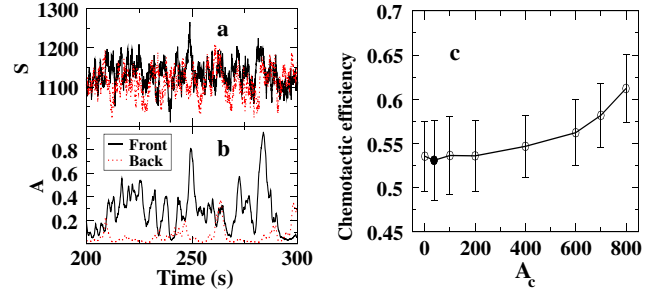

FIG. 3 (color online). Example of the input signal (a) and the output signal of balanced inactivation model (b). Parameter values are $A_c = 0$, $\tau_a = 1.3$ s, $k_a = 0.01$ s^{-1}, $k_i = 1000$ μm (s molecule)$^{-1}$, $k_b = 3$ μm s^{-1}, $k_{-a} = 0.2$ s^{-1}, $k_{-b} = 0.2$ s^{-1} and $D = 10$ μm^2 s^{-1}. The distance between the front and the back is $L = 10$ μm, $p = 0.01$, $K_d = 30$ nM and $c = 1$ nM. (c) The chemotactic efficiency as a function of the amplitude of the noise cross-correlation. The solid point corresponds to the amplitude found using the MCell simulation and represents a typical experimental value. Parameter values are as above and in Fig. 1 with $T_{dec} = 30$ s, $T_{int} = 10$ s and $\theta = 0.95$.

the cell). Similar expressions hold for C_{bb}. The cross-correlation was found to fit the expression $C_{fb} = \frac{A_c}{\tau_c} t e^{-t/\tau_c}$ with both A_c and τ_c as fitting parameters.

An efficient way to generate the required noise spectra can be formulated using the Fourier transform of the fits to the auto and cross correlation:

$$\tilde{C}_{ff}(\omega) = \frac{2A_a/\tau_a}{1/\tau_a^2 + \omega^2}; \qquad \tilde{C}_{fb}(\omega) = \frac{2A_c(1/\tau_c^2 - \omega^2)}{\tau_c(1/\tau_c^2 + \omega^2)^2}. \tag{4}$$

Gaussian distributed random variables were drawn from this spectrum and were used to calculate the corresponding spectra for B. The time series of B were obtained using inverse Fourier transforms and substituted into the equations for the membrane-bound components of the directional sensing model. These ODEs (one for the back and one for the front) are then solved numerically. An example of the resulting time traces is shown in Fig. 3(a) for the signal at the front and the back and 3(b) for the corresponding output of the directional sensing model. Clearly, even though the balanced inactivation model is able to filter out some of the noise of the input signal, the output signal remains noisy.

To quantify the output of the directional sensing model, and thus to generate a measure for motility of the cell, we constructed a motility model that uses the difference in A at the front and the back, normalized by the mean, to decide to move up or down the gradient. This simplified model ignores all the complex and largely unknown steps between directional sensing and motility including the cytoskeleton machinery. Specifically, we calculate

$$G(t) = \frac{\int_{-\infty}^{t} e^{(t-s)/T_{int}}(A_f - A_b)ds}{\int_{-\infty}^{t} e^{(t-s)/T_{int}}(A_f + A_b)ds} \tag{5}$$

after each "decision" interval T_{dec} and where we have introduced the integration time T_{int}. Motivated by typical pseudopod lifetimes in *Dictyostelium* we choose $T_{dec} = 30$ s and $T_{int} = 10$ s although similar qualitative results

were obtained using different values. The cell takes a positive unit step in the direction of the gradient if G is larger than a threshold θ, takes a negative unit step in the "wrong" direction if G is smaller than this threshold and does not move if $-\theta \leq G \leq \theta$. The chemotactic efficiency CE is then defined as the total displacement in the direction of the gradient divided by the total number of decision intervals and can take on values between -1 and $+1$. We note that defining an alternative measure of the chemotactic efficiency using the SNR of $A_f - A_b$ ([4,5]) leads to qualitatively similar results.

We have first determined the relative importance of the cross correlation. For this, we fixed the amplitude and time scale of the autocorrelation and determined CE as a function of the amplitude of the cross correlation A_c. An example of such a simulation is shown in Fig. 3(c) for a particular set of parameters. The error bars correspond to a standard deviation obtained by running 100 simulations of 5000 s each. The value of the cross correlation indicated by the solid symbol is the one found using the parameters values for *Dictyostelium* of Fig. 2. This graph demonstrates that the cross-correlation affects CE by at most 4% and that for biological realistic values the contribution of the cross correlation can be safely ignored. We have verified that this result does not depend strongly on the chosen parameters.

Next, we determined CE as a function of the gradient steepness, setting $A_c = 0$. The result can be found in Fig. 4(a) and shows that CE increases as the steepness increases. This, of course, can be expected since an increase in gradient steepness leads to an increasing difference in the number of bound receptors at the front and the back. A qualitatively similar sigmoidal dependence was found for different values of the model parameters.

We also determined CE as a function of the autocorrelation time τ_a. Consistent with studies on the propagation
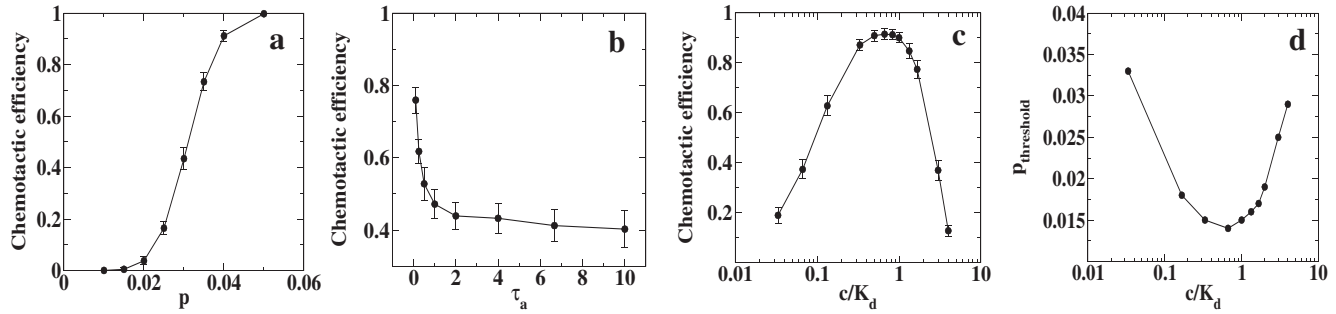
FIG. 4.　The chemotactic efficiency as a function of the steepness of the gradient (a), the autocorrelation time scale (b) and the background concentration (c). Fixed parameter values are as in Fig. 3 and 4 with $\theta = 0.95$ (a), $p = 0.01$ and $\theta = 0.65$ (b) and $\tau_{\text{diff}} = 0.3$ s, $p = 0.01$ and $\theta = 0.85$ (c). In (d) we have plotted the onset of chemotaxis, defined as a CE value larger that 0.5, as a function of the background concentration ($\tau_{\text{diff}} = 0.3$ s and $\theta = 0.95$).

of noise in signal transduction networks [3,17] the result demonstrates that a larger correlation time is detrimental to detecting the gradient [Fig. 4(b)]. Conversely, the maximum CE a cell can achieved for a given set of parameters is in the white noise limit $\tau_a \rightarrow 0$. This result could be tested experimentally using the explicit expression for the correlation time [Eq. (3)]. For example, decreasing the diffusion constant of the ligands via chemical modifications by a factor of 10 would increase the correlation time roughly threefold. This increase is predicted to lead to a decrease in the chemotactic efficiency.

Finally, we determined CE as a function of the background concentration. The results, shown in Fig. 4(c), demonstrate that CE exhibits a clear maximum around $c/K_d \sim 0.7$. Although we have not performed a systematic parameter sweep, it appears that the observed maximum varies only slightly for different directional sensing and motility parameters and occurs consistently for $c/K_d \lesssim 1$. It should be possible to experimentally test this prediction using microfluidic devices similar to the ones used in Ref. [2]. In particular, the minimum gradient for chemotaxis should be a function of the background concentration much like our numerical results shown in Fig. 4(d).

In summary, we have presented an efficient way to calculate the effect of receptor noise levels on the gradient sensing capabilities of eukaryotic cells. We were able to derive analytical expressions for the diffusive cytosolic inhibitor that depend on the auto- and cross-correlation spectra of the receptor occupancy. Through direct numerical calculations, we found that the contribution of the cross-correlation to motility can be neglected. Our method is directly applicable to other directional sensing models in which a diffusing species is linearly generated by the external signal [14]. However, we point out that for more complicated directional sensing models for which the diffusion equation is not diagonal in frequency space one can always directly integrate the underlying equations. Future directions currently underway include investigations in higher dimensions, where preliminary results show that

the qualitative features remain unchanged, and the inclusion of noise terms in the signal transduction pathway.

[1] P. J. V. Haastert and P. N. Devreotes, Nat. Rev. Mol. Cell Biol. **5**, 626 (2004).

[2] L. Song, S. M. Nadkarni, H. U. Bödeker, C. Beta, A. Bae, C. Franck, W.-J. Rappel, W. F. Loomis, and E. Bodenschatz, Eur. J. Cell Biol. **85**, 981 (2006).

[3] T. Shibata and K. Fujimoto, Proc. Natl. Acad. Sci. U.S.A. **102**, 331 (2005).

[4] M. Ueda and T. Shibata, Biophys. J. **93**, 11 (2007).

[5] P. J. van Haastert and M. Postma, Biophys. J. **93**, 1787 (2007).

[6] B. W. Andrews and P. A. Iglesias, PLoS Comput. Biol. **3**, 153(E) (2007).

[7] P. Herzmark, K. Campbell, F. Wang, K. Wong, H. El-Samad, A. Groisman, and H. R. Bourne, Proc. Natl. Acad. Sci. U.S.A. **104**, 13 349 (2007).

[8] H. Meinhardt, J. Cell Sci. **112**, 2867 (1999).

[9] A. Gamba, A. de Candia, S. D. Talia, A. Coniglio, F. Bussolino, and G. Serini, Proc. Natl. Acad. Sci. U.S.A. **102**, 16 927 (2005).

[10] M. Postma and P. J. M. van Haastert, Biophys. J. **81**, 1314 (2001).

[11] A. Narang, K. K. Subramanian, and D. A. Lauffenburger, Ann. Biomed. Eng. **29**, 677 (2001).

[12] H. Levine, D. A. Kessler, and W. J. Rappel, Proc. Natl. Acad. Sci. U.S.A. **103**, 9761 (2006).

[13] C. A. Parent and P. N. Devreotes, Science **284**, 765 (1999).

[14] A. Levchenko and P. A. Iglesias, Biophys. J. **82**, 50 (2002).

[15] J. R. Stiles and T. M. Bartol, in *Computational Neurobiology: Realistic Modeling for Experimentalists*, edited by E. de Schutter (CRC Press, Boca Raton, FL, 2001).

[16] K. Wang, W. J. Rappel, R. Kerr, and H. Levine, Phys. Rev. E **75**, 061905 (2007).

[17] J. Paulsson, Nature (London) **427**, 415 (2004).